Enhancing Near-Infrared Spectroscopy Analysis Using Ordinal Pattern Methods

Quentin Legros, Brieuc Léger, Pascal Auzou, Canan Ozsancak, Julien Bonnal and Meryem Jabloun

***Abstract*—This paper presents a novel approach for automatic hemodynamic response detection in functional Near-Infrared Spectroscopy (fNIRS) signals, a modern neuroimaging technique that offers a portable and non-invasive solution for monitoring brain activity in naturalistic settings. We address the challenges posed by signal complexity and inter-subject variability by leveraging two entropy-based methods, Permutation Entropy (PE) and Phase Rectified Signal Average (PRSA), which focus on the statistical properties of noise rather than the signal content itself. Our experiments on raw, annotated fNIRS recordings data demonstrate that these methods achieve performance comparable to traditional machine learning algorithms, with the additional advantage of requiring no prior training. Their versatility, adaptability to various signal types, and significant reduction in computational time make them particularly well-suited for real-time applications in dynamic environments, further enhancing the practical potential of fNIRS in cognitive and clinical research.**

***Index Terms*—fNIRS signals, Signal processing, Ordinal method, Machine Learning, Entropy**

I. Introduction

Functional Near-Infrared Spectroscopy (fNIRS) is a non-invasive neuroimaging technique that has gained significant attention for its ability to monitor brain activity in real-time [1], [2]. Unlike other neuroimaging techniques such as Functional Magnetic Resonance Imaging (fMRI), Magnetoencephalography (MEG), and Electroencephalography (EEG), fNIRS uses near-infrared light to detect changes in hemoglobin concentration, and offer a portable, cost-effective, and accessible alternative. fNIRS has proven to be valuable in various fields, including cognitive neuroscience, clinical rehabilitation, and brain-computer interfaces [3], particularly in applications requiring real-time monitoring.

Despite the availability of commercial software tools for fNIRS signal analysis, current methodologies often fail to fully capture the complexity of the data [4]. Many existing methods rely on oversimplified assumptions or are limited by preprocessing steps (such as denoising or bandpass filtering), which may overlook important aspects of the signal [1], [4]. Moreover, the presence of confounding factors such as Mayer waves, respiratory fluctuations, and cardiac interference further complicates traditional approaches, often making it difficult to separate meaningful hemodynamic responses from other physiological signals or noise.

Q. Legros (quentin.legros@univ-orleans.fr) and M. Jabloun are with the PRISME Laboratory, Orléans University, Orléans 45072, France. P. Auzou, C. Ozsancak, B. Léger and J. Bonnal are with the LIRSO Laboratory, CHU d'Orléans, 45100, France.

While Machine Learning (ML) and Deep Learning (DL) models have shown promising results in fNIRS signal analysis [5], these methods require large datasets for training, which is challenging due to the evolving nature of fNIRS technology and advancements in sensor hardware [6]. Additionally, these models often lack interpretability, making it difficult to understand the underlying reasons for certain patterns in the data [5], and the need for retraining with each hardware update reduces their practicality for real-time applications [7].

To address these limitations, this paper presents an alternative approach for analyzing fNIRS signals that operates directly on the raw intensity data, bypassing the need for complex preprocessing steps. Our approach focuses on detecting the presence or absence of hemodynamic responses using ordinal pattern (OP)-based methods, which are less sensitive to the challenges posed by noise and interference in the signal. Specifically, we explore the use of Permutation Entropy (PE) and Phase-Rectified Signal Averaging (PRSA) [8], [9], which focus on the statistical properties of noise and randomness in the data rather than specific signal features. These methods offer advantages in terms of low computational cost, high efficiency, and robustness to noise commonly present in fNIRS signals.

The paper is structured as follows: Section II introduces fNIRS signals and study objectives. The OP-based methods are presented in Section III for PRSA, PE, and two other variants of PE. Section IV defines the decision rules for detecting hemodynamic responses. Section V provides a comparative analysis, and Section VI summarizes the findings.

II. Functional Near-Infrared Spectroscopy

Functional Near-Infrared Spectroscopy (fNIRS) records the intensity of two near-infrared wavelengths transmitted through the scalp; absorption differences between oxygenated (HbO) and deoxygenated (HbR) haemoglobin modulate this intensity and thus reflect neural activation [1]. These variations are influenced by the optical properties of the blood, primarily the absorption characteristics of hemoglobin, which varies depending on its oxygenation state [1]. The resulting changes in HbO and HbR concentrations reflect neural activity [1].

The acquisition of fNIRS signals typically involves alternating between resting and active periods, providing information on the dynamics of brain function. A key challenge in analyzing these signals is differentiating meaningful brain activity from noise, particularly in detecting Hemodynamic Responses (HR) that reflect neural activation [1].

Let $x[n]$ denote the raw signal, representing the intensity of light detected by the sensors at the discrete-time index

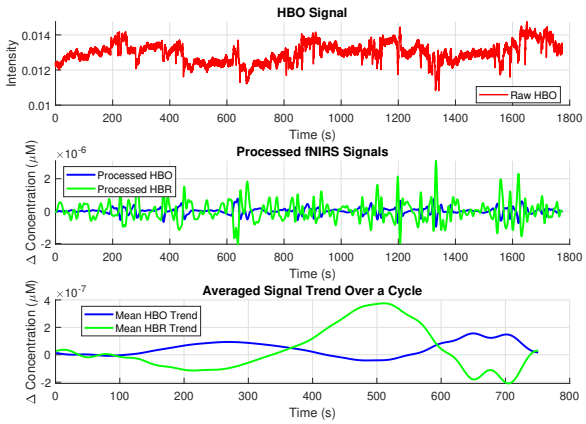

Fig. 1. fNIRS signal processing. (Top) Raw fNIRS signal representing light intensity variations over time. (Middle) Estimated HbO and HbR concentrations obtained from the raw signal using the modified Beer-Lambert law. (Bottom) Block-averaged hemodynamic response computed across each cycle of activity, improving signal clarity and reducing noise.

n. The raw signal $x[n]$ is influenced by both the absorption and scattering of light within brain tissue, as well as by the source-detector geometry [1]. The standard approach involves converting $x[n]$ into optical density $\mu[n]$, typically using the Beer-Lambert law [10]:

$$\mu[n] = -\log\left(\frac{x[n]}{x_0}\right), \tag{1}$$

where x_0 is the incident intensity of the light emitted by the source. The optical density $\mu[n]$ emphasizes the attenuation of light due to absorption and scattering as it travels through biological tissues. The standard fNIRS pipeline computes HbO and HbR from optical density, and often resort to preprocessing steps such as bandpass filtering, baseline correction and denoising [10]. However, the lack of standardization in these steps introduces variability, compromising the interpretability and reproducibility of the results [2], [5], [11].

In this paper, we focus exclusively on the raw signal $x[n]$ without additional assumptions, avoiding uncertainties introduced by preprocessing HbO and HbR concentrations. However, raw fNIRS data are often affected by noise, including motion artifacts and sensor drift, posing a challenge for accurate analysis. Addressing these noise-related challenges is essential to ensure reliable interpretations of fNIRS signals [6].

As shown in Fig 1, the raw signal $x[n]$ is first obtained, which represents light intensity variations over time (Top). This signal is then converted into optical density $\mu[n]$, and further processed to estimate the concentrations of oxygenated (HbO) and deoxygenated hemoglobin (HbR), as shown in the middle subplot of Fig. 1 (Middle). The final step involves reducing noise and improving signal clarity through, for instance, a block averaging process (see Fig. 1 Bottom).

Another challenge is automating fNIRS analysis to improve efficiency and reduce the time experts spend on manually assessing noisy data, allowing them to focus on critical aspects [2]. An additional challenge, and not the least important, is the lack of large, high-quality publicly available fNIRS datasets, probably due to the early stage of fNIRS technology and rapidly evolving hardware [4]. Currently, only a small number of dataset is currently open access [12], [13]. This challenge actually limits the recent advancements in ML and DL, which, despite their potential to automate fNIRS data analysis, have shown limited generalization and little insight into the physiological processes driving changes in hemoglobin concentrations [1]. Additionally, the frequent need for model retraining to adapt to hardware changes makes these approaches computationally expensive and impractical for real-time applications.

III. Ordinal Pattern (OP)-based method

This section focuses on OP-based methods, specifically PRSA and PE variants, for processing raw fNIRS signals. These methods effectively capture hidden dynamics within noisy data while requiring minimal preprocessing and assumptions. Their support for real-time processing also makes them highly suitable for practical applications [2]. Building on these techniques, we aim to develop an efficient, robust, and fast approach for detecting hemodynamic responses in fNIRS signals, thereby enhancing non-invasive brain activity detection.

A. Permutation Entropy

Permutation Entropy (PE) is a complexity measure designed to quantify the disorder or randomness in a signal by analyzing its temporal structure[1] [8]. Given a time series $x[n]$, PE is computed by embedding this signal into a higher-dimensional phase space using d-dimensional subsequences with a time delay τ:

$$\Big[x[n], x[n+\tau], \ldots, x[n+\tau(d-1)]\Big]. \tag{2}$$

The relative order of values within each subsequence defines an ordinal pattern (OP), with a total of $d!$ possible patterns. For example, when $d = 2$ and $\tau = 0$, there are two possible OPs: 01 if $x[n] < x[n+1]$ and 10 otherwise. The frequency of occurrence of each OP, denoted p_i where $i = 1, 2, \ldots, d!$, is used to calculate the Shannon entropy. Formally, the normalized PE is defined as:

$$H_{PE}(d, \tau) = -\frac{1}{\log(d!)} \sum_{i=1}^{d!} p_i \log(p_i), \tag{3}$$

ensuring that the PE values range from 0 (perfect order) to 1 (maximum disorder) [8].

The parameters d and τ play a crucial role in determining the scale and sensitivity of the complexity measure. The embedding dimension d should be chosen based on the complexity of the signal, where higher dimensions can capture

[1]Recurrence plots also analyse temporal structure but rely on pairwise distance calculations in the reconstructed phase space, leading to quadratic complexity. Permutation-based entropies use only ordinal information and therefore scale linearly with signal length, which is preferable for real-time fNIRS.

more intricate patterns. Typically, values between 2 and 10 are used, depending on the signal's characteristics [8].

In practice, PE can be computed for different time scales or embedding dimensions, providing a range of values that reflect the signal's complexity across these scales. For instance, as the embedding dimension increases, the entropy will generally increase, reflecting the increased complexity of the signal's structure. By varying both d and τ, one can obtain a more nuanced understanding of the signal's temporal dynamics.

PE and its extensions are valuable tools for analyzing the complexity of physiological signals [14], as they detect changes in their temporal structure. Figure 2 shows that PE decreases as the Signal-to-Noise Ratio (SNR) increases, indicating greater regularity of the signal. This ability to quantify signal order makes PE a promising approach for detecting meaningful brain activity amid noise, particularly in fNIRS applications, where both periodic and irregular patterns can be obscured by noise [15]. To improve the detection of hidden structures in hemodynamic responses measured by fNIRS, we propose hereafter two additional PE variants.

Slope Entropy (SE): quantifies the PE of the signal derivative, incorporating amplitude information that is typically discarded in the original PE formulation [16]. SE is particularly sensitive to rapid changes in the signal, capturing fast-varying dynamics. Sharp transitions or fluctuations result in higher SE values, indicating greater complexity, while smooth signals with gradual changes yield lower SE values.

Refined Composite Downsampling (rcdPE): is an extension of PE that applies a downsampling procedure for multiscaling [17]. It constructs downsampled signals with different starting points, enhancing precision and sensitivity to hidden dynamic variations. rcdPE provides a series of PE values computed at different time scales, returning a vector of size $M_{\max}$, where $M_{\max}$ is the maximum time scale to analyze. This multiresolution analysis helps capture both short-term and long-term dynamics that might be missed in a standard PE analysis. Additionally, rcdPE avoids artifact cross-correlation, a limitation present in other multiscale PE extensions, by ensuring that the downsampling process is more robust.

Thus, PE, SE, and rcdPE not only provide a single value of complexity but also return a series of values that depend on the embedding dimension and time scale, allowing a more detailed analysis of how complexity evolves across different scales of the signal.

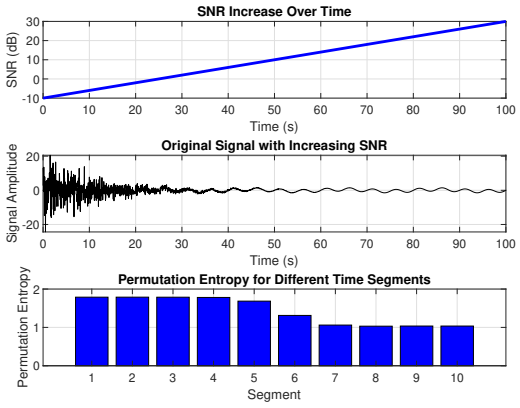

Fig. 2. PE applied to a synthetic sinusoid with additive Gaussian noise. Top: SNR forced to rise linearly from 0 dB to 10 dB. Middle: noisy signal, $f_s = 25$ Hz. Bottom: non-normalised PE for successive windows ($d = 3,\ \tau = 5$); PE falls as SNR improves, illustrating increasing regularity.

B. Phase-Rectified Signal Averaging

The Phase-Rectified Signal Averaging (PRSA) method was introduced in [18] and can be viewed as an OP concept combined with phase-synchronized averaging [9], [18]. While PE-based metrics capture instantaneous complexity, PRSA exploits phase-aligned averaging to boost SNR and reveal slower, coherent haemodynamic responses that may be missed by purely entropy-based measures. For classification we use the variance of the PRSA curve, denoted σ^2_{PRSA}, as a single scalar feature. Its main steps are described in Algorithm 1.

Algorithm 1 PRSA Steps for fNIRS Signal Processing

1: **Input:** A raw signal $x[n]$ and a delay τ.
2: Identify the most frequent OP of length d within $x[n]$, denoted as Π.
3: Locate M anchor points $\{n_i\}_{i=1:M}$ where segments $\{x[n_i], \ldots, x[n_i + d - 1]\}$ match OP type Π.
4: Extract M segments of length $2L + 1$ centered on anchor points:

$$S_i = \{x[n_i - L],\ x[n_i - L + 1], \ldots,\ x[n_i], \ldots,\ x[n_i + L]\}.$$

5: Perform phase synchronization by aligning and averaging the M segments:

$$X_{\text{PRSA}}[k] = \frac{1}{M} \sum_{i=1}^{M} x[n_i + k], \quad -L \le k \le L.$$

6: **Output:** The PRSA signal $X_{\text{PRSA}}[k]$.

Through phase-synchronized averaging, PRSA enhances structured signal components with phase coherence across multiple signal segments while suppressing uncorrelated noise [9]. More precisely, consider the raw signal model: $x[n] = s[n] + \epsilon[n]$, where $s[n]$ is the signal of interest, and $\epsilon[n]$ represents an i.i.d. noise. As the number of anchor points N increases, PRSA reduces the noise component, improving the Signal-to-Noise Ratio (SNR):

$$\text{SNR}_{PRSA} \approx \frac{\mathbb{E}\left[s[n]^2\right]}{\frac{1}{M}\mathbb{E}\left[\epsilon[n]^2\right]}. \tag{4}$$

This makes PRSA particularly attractive for fNIRS application, where weak hemodynamic responses are often masked by noise. Its ability to improve SNR is essential for accurate brain activity analysis. Figure 3 illustrates PRSA applied to a sinusoidal signal embedded in additive centered Gaussian noise, where the SNR increases from 0 dB to 10 dB over time. The noisy signal is shown in the upper plot, while the PRSA curves for different SNR levels (0 dB, 5 dB and 10 dB) are displayed in the lower plot. As the SNR improves,

the PRSA curve becomes smoother and more sinusoidal, indicating effective noise suppression while preserving the structured components of the signal.

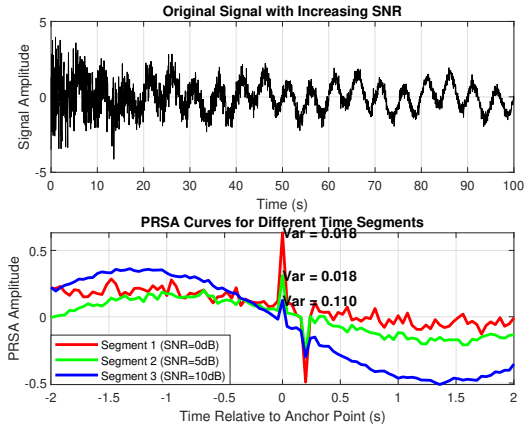

Fig. 3. PRSA with $d = 2$ and $L = 50$ applied to simulated noisy sinusoids sampled at $fs = 25$Hz with increasing SNR. The first subplot shows a noisy signal with an increasing SNR from 0 dB to 10 dB over time. The second subplot presents PRSA curves for different SNR levels (0 dB, 5 dB, and 10 dB).

IV. Decision Rules for Detecting Hemodynamic Responses

We define specific decision criteria for detecting HR associated with cerebral activity. PRSA identifies a significant HR when σ^2_{PRSA} exceeds 0.05, distinguishing meaningful responses from noise. For entropy-based methods, HR detection is based on the mean entropy values over their respective vectors.

For PE, HR is detected when the entropy value is less than or equal to 0.7, indicating a more ordered signal. For SE, HR is detected when the mean entropy value across all embedding dimensions is greater than or equal to 0.7, as higher entropy reflects dynamic local changes. Similarly, for rcdPE, HR is detected when the mean entropy value across all downsampling scales is less than or equal to 0.7, capturing complexity reduction at multiple scales.

These threshold values were empirically determined using deterministic test signals embedded in additive Gaussian noise.

V. Experimental Setup and Results

This section evaluates the considered OP-based methods[2] for detecting the presence or absence of HR in fNIRS signals.

A. Experimental setup

fNIRS dataset - We use the publicly available NiReject Benchmark dataset that consists of multi-participant recordings of raw optical intensity measurements captured using a multi-channel fNIRS system. Although extraction of HbO and HbR concentrations is provided, our analysis focuses exclusively on raw signals to evaluate the competing methods. Raw signals preserve all original information from the fNIRS system, maintaining variations that may be lost during preprocessing steps [2].

Hyper-parameter selection. Each method relies on a small set of hyper-parameters. We tuned them by a five-fold subject-wise cross-validation: in each fold 80 % of the subjects are used for training and parameter tuning (grid search inside this split) and the remaining 20 % for testing. The explored ranges were $d \in \{2, \ldots, 6\}$ and $\tau \in \{1, \ldots, 10\}$ for all PE-based metrics, and $L \in \{16, 32, 48, 64\}$ for PRSA. The values maximising balanced accuracy are reported in Table I. A sensitivity analysis shows that changing d or τ by ± 1 around these settings alters the final accuracy by < 1 percentage point, indicating that the methods are not critically tuned.

TABLE I
HYPER-PARAMETERS RETAINED AFTER CROSS-VALIDATION.

Method	d	Other parameter	Note
PE	2	$\tau = 1$	–
SE	4	$m_{\max} = 4,\ \tau = 1$	amplitude info
rcdPE	3	$M_{\max} = 4,\ \tau = 1$	multiscale
PRSA	4	$L = 32$	window length

Benchmark Methods - To assess the performance of the OP-based methods in detecting the presence or absence of HR in fNIRS signals, the classification accuracy using the decision rules detailed in Section IV is used as a performance metric. As benchmarks, we employ Support Vector Machines (SVM) [6], [19] and Random Forest classifiers, both commonly used methods for activity detection in fNIRS data [6], [19], [20]. The SVM is trained on 80% of the R22 subset of the NiReject Benchmark dataset and tested on the remaining 20%. Similarly, the Random Forest classifier is trained on the same subset using 100 decision trees.

B. Results on fNIRS signals

The results are summarized in Table II. The results demonstrate that almost all entropy-based methods (PE, rcdPE and PRSA) achieve accuracy comparable to SVM and Random Forest, confirming their effectiveness in detecting HRs. Among the entropy–based methods, both PE and rcdPE achieved the best accuracy (95.89%), underscoring their ability to distinguish meaningful signal content from noise. While SE also performed well, its sensitivity to rapid signal variations may explain minor accuracy discrepancies.

Method	**Accuracy**	**Computational Time (sec)**
PRSA	95.82%	$3.20 \cdot 10^{-3}$
PE	95.89%	$2.12 \cdot 10^{-4}$
SE	86.25%	$2.11 \cdot 10^{-4}$
rcdPE	95.89%	$3.22 \cdot 10^{-4}$
SVM (training)	N/A	3.36
SVM (inference)	95.81%	0.28
Random Forest (training)	N/A	12.03
Random Forest (inference)	96.14%	0.34

TABLE II
PERFORMANCE METRICS: ACCURACY (%) AND COMPUTATIONAL TIME FOR DIFFERENT METHODS.

[2]MATLAB code is freely available at https://github.com/QuentinLEGROS/fNIRS2025

Moreover, the lower performance of SE compared to PE and rcdPE may be attributed to its sensitivity to amplitude variations in addition to symbolic patterns. Since raw fNIRS signals are often affected by physiological artifacts such as respiration and motion-induced intensity fluctuations, SE might capture these unwanted variations rather than purely reflecting the underlying hemodynamic response.

Note that inter-subject variability poses a challenge in fNIRS-based classification, yet the stable performance of entropy-based methods across the dataset suggests strong generalization capabilities.

As shown in Table II, PE and SE require the least computational time (2.1×10^{-4} sec per realization), whereas rcdPE and PRSA demand slightly more processing power. By contrast, SVM and Random Forest are significantly slower, with Random Forest requiring 12.03 sec for training and 0.34 sec for inference, making it the most computationally intensive approach.

Entropy-based methods offer an additional advantage over SVM and Random Forest: they achieve similar accuracy without requiring training or feature selection, making them well-suited for real-time applications. Their robustness to noise and artifacts further enhances their applicability, as they operate directly on raw signals without extensive preprocessing.

VI. Conclusion

In this study, we presented entropy-based methods, specifically PE, its variants and PRSA, for detecting hemodynamic responses in fNIRS signals. Our results show that while Random Forest achieves slightly higher accuracy, entropy-based methods such as PE and rcdPE offer comparable performance. These methods have the added advantage of requiring minimal computational time, with PE and SE requiring only 2.1×10^{-4} sec per realization, making them highly efficient for real-time applications.

Entropy-based methods do not require training or feature selection, distinguishing them from traditional machine learning models like SVM and Random Forest. This simplifies their deployment, especially in dynamic environments where hardware and signal properties may change over time. Their robustness to noise and the fact that they operate directly on raw intensity signals further increase their practical applicability, as they bypass the need for extensive preprocessing.

Future work will focus on optimizing these methods for even faster real-time processing and exploring adaptive threshold selection to further improve accuracy across diverse fNIRS signal conditions. Automating threshold selection is particularly relevant given the variability of hemodynamic responses and noise levels, ensuring better generalization across subjects and experimental settings.

References

[1] S. Baunce, M. Izzetoglu, K. Izzetoglu, B. Onaral, and K. Pourrezae, "Functional near-infrared spectroscopy. An emerging neuroimaging modality," *IEEE engineering in medicine and biology magazine*, pp. 54–62, 2006.

[2] F. Herold, P. Wiegel, F. Scholkmann, and N. G. Müller, "Applications of functional near-infrared spectroscopy (fNIRS) neuroimaging in exercise–cognition science: a systematic, methodology-focused review," *Journal of clinical medicine*, vol. 7, no. 12, p. 466, 2018.

[3] J. Bonnal, C. Ozsancak, F. Prieur, and P. Auzou, "Video mirror feedback induces more extensive brain activation compared to the mirror box: an fNIRS study in healthy adults," *Journal of NeuroEngineering and Rehabilitation*, vol. 21, no. 1, p. 78, 2024.

[4] S. Brigadoi, L. Ceccherini, S. Cutini, F. Scarpa, P. Scatturin, J. Selb, L. Gagnon, D. A. Boas, and R. J. Cooper, "Motion artifacts in functional near-infrared spectroscopy: a comparison of motion correction techniques applied to real cognitive data," *Neuroimage*, vol. 85, pp. 181–191, 2014.

[5] Z. Cao and Z. Luo, "Calibration of deep learning classification models in fNIRS," *arXiv preprint arXiv:2402.15266*, 2024.

[6] N. Naseer and K.-S. Hong, "fNIRS-based brain-computer interfaces: a review," *Frontiers in human neuroscience*, vol. 9, p. 3, 2015.

[7] J. Benerradi, J. Clos, A. Landowska, M. F. Valstar, and M. L. Wilson, "Benchmarking framework for machine learning classification from fNIRS data," *Frontiers in Neuroergonomics*, vol. 4, p. 994969, 2023.

[8] C. Bandt and B. Pompe, "Permutation entropy: a natural complexity measure for time series," *Physical review letters*, vol. 88, no. 17, p. 174102, 2002.

[9] A. Bauer, P. Barthel, A. Müller, J. Kantelhardt, and G. Schmidt, "Bivariate phase-rectified signal averaging—a novel technique for cross-correlation analysis in noisy nonstationary signals," *Journal of electrocardiology*, vol. 42, no. 6, pp. 602–606, 2009.

[10] L. Kocsis, P. Herman, and A. Eke, "The modified Beer–Lambert law revisited," *Physics in Medicine & Biology*, vol. 51, no. 5, p. N91, 2006.

[11] F. Herold, P. Wiegel, F. Scholkmann, A. Thiers, D. Hamacher, and L. Schega, "Functional near-infrared spectroscopy in movement science: a systematic review on cortical activity in postural and walking tasks," *Neurophotonics*, vol. 4, no. 4, pp. 041403–041403, 2017.

[12] C. Gerloff, M. A. Yücel, L. Mehlem, K. Konrad, and V. Reindl, "NiReject: toward automated bad channel detection in functional near-infrared spectroscopy," *Neurophotonics*, vol. 11, no. 4, pp. 045008–045008, 2024.

[13] Z. Huang, L. Wang, G. Blaney, C. Slaughter, D. McKeon, Z. Zhou, R. Jacob, and M. C. Hughes, "The tufts fNIRS mental workload dataset & benchmark for brain-computer interfaces that generalize," in *Thirty-fifth Conference on Neural Information Processing Systems Datasets and Benchmarks Track (Round 2)*, 2021.

[14] M. Zanin, L. Zunino, O. A. Rosso, and D. Papo, "Permutation entropy and its main biomedical and econophysics applications: a review," *Entropy*, vol. 14, no. 8, pp. 1553–1577, 2012.

[15] S. Keshmiri, "Entropy and the brain: An overview," *Entropy*, vol. 22, no. 9, p. 917, 2020.

[16] D. Cuesta-Frau, "Slope entropy: A new time series complexity estimator based on both symbolic patterns and amplitude information," *Entropy*, vol. 21, no. 12, p. 1167, 2019.

[17] A. Dávalos, M. Jabloun, P. Ravier, and O. Buttelli, "Improvement of statistical performance of ordinal multiscale entropy techniques using refined composite downsampling permutation entropy," *Entropy*, vol. 23, no. 1, p. 30, 2020.

[18] A. Bauer, J. Kantelhardt, P. Barthel, R. Schneider, M. Mäkikallio, H. Huikuri, and G. Schmidt, "Deceleration capacity of heart rate as a predictor of mortality after myocardial infarction: cohort study," *The Lancet*, vol. 367, no. 9523, pp. 1674–1681, 2006.

[19] R. Fernandez Rojas, X. Huang, and K.-L. Ou, "A machine learning approach for the identification of a biomarker of human pain using fNIRS," *Scientific reports*, vol. 9, no. 1, p. 5645, 2019.

[20] J. Gemignani, "Classification of fNIRS data with LDA and SVM: a proof-of-concept for application in infant studies," in *2021 43rd Annual International Conference of the IEEE Engineering in Medicine & Biology Society (EMBC)*, pp. 824–827, IEEE, 2021.